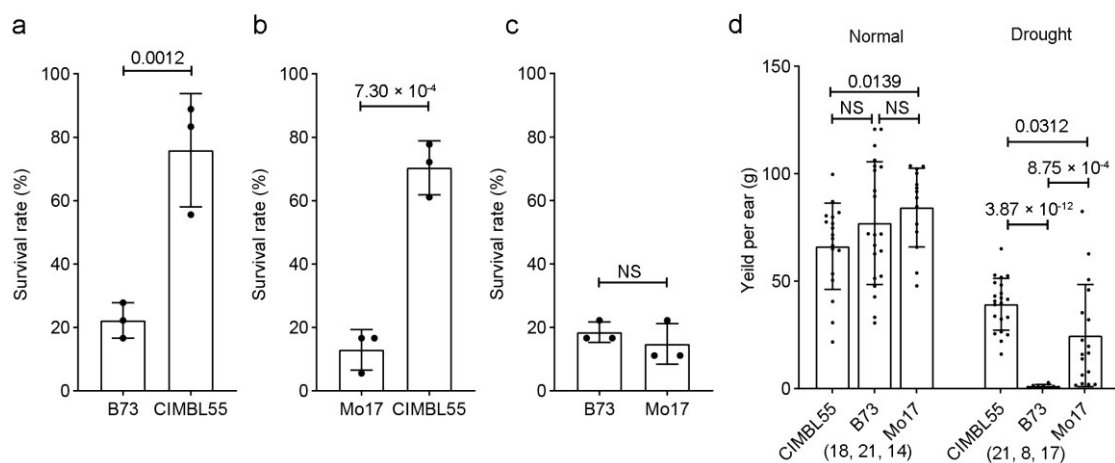
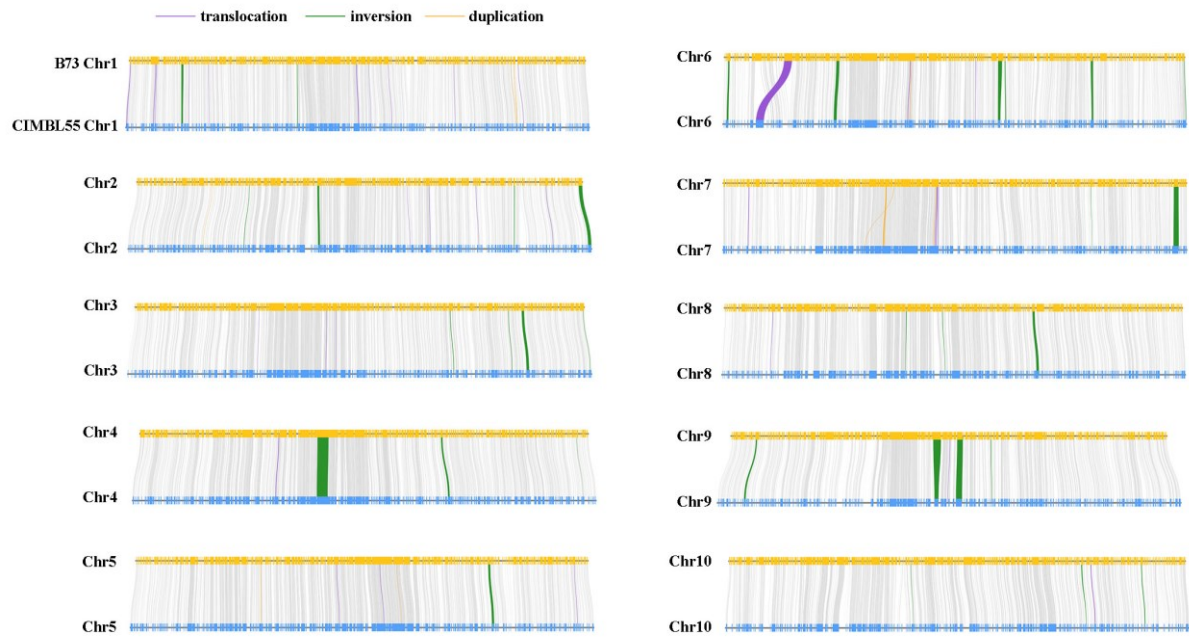


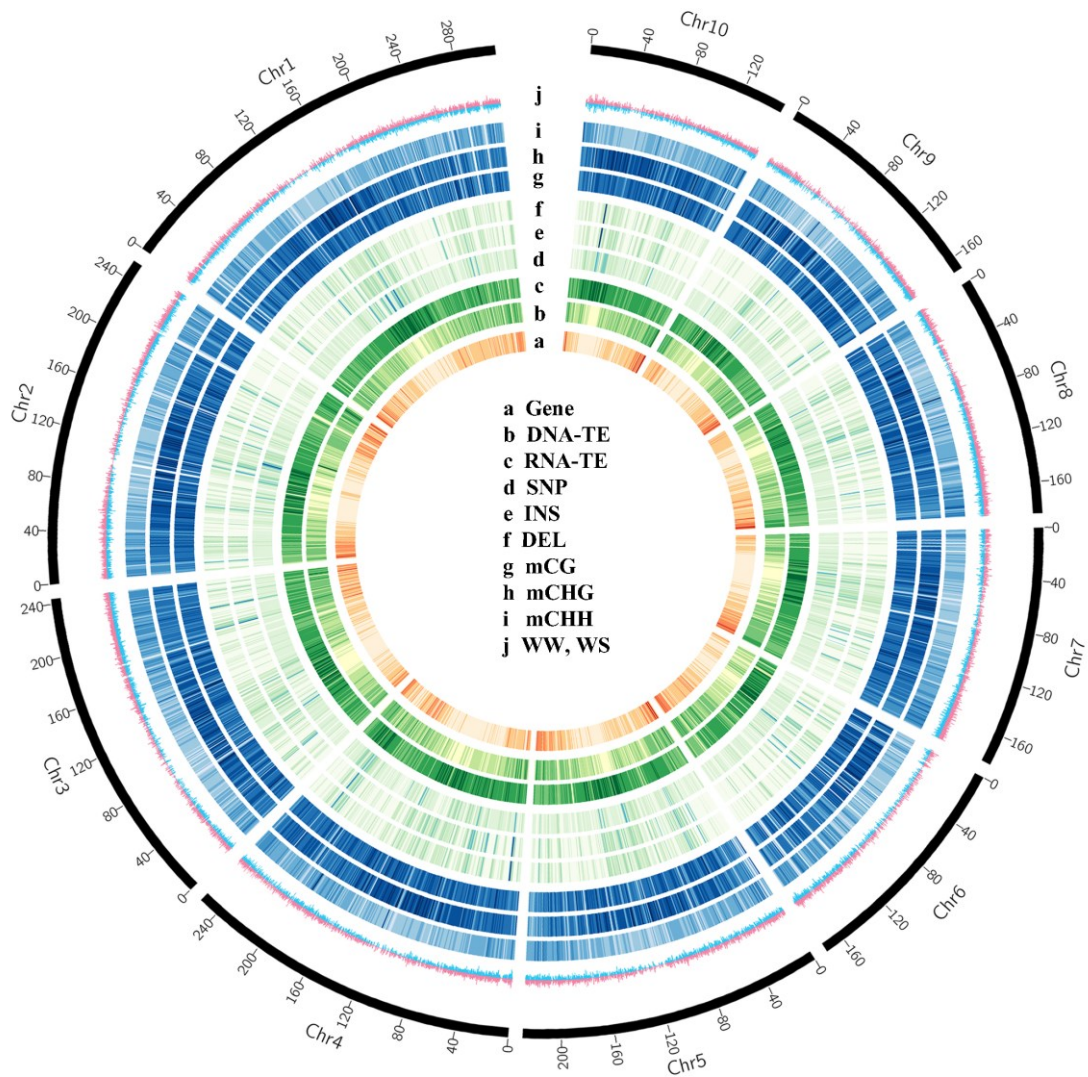
SUPPLEMENTARY FIGURES AND LEGENDS



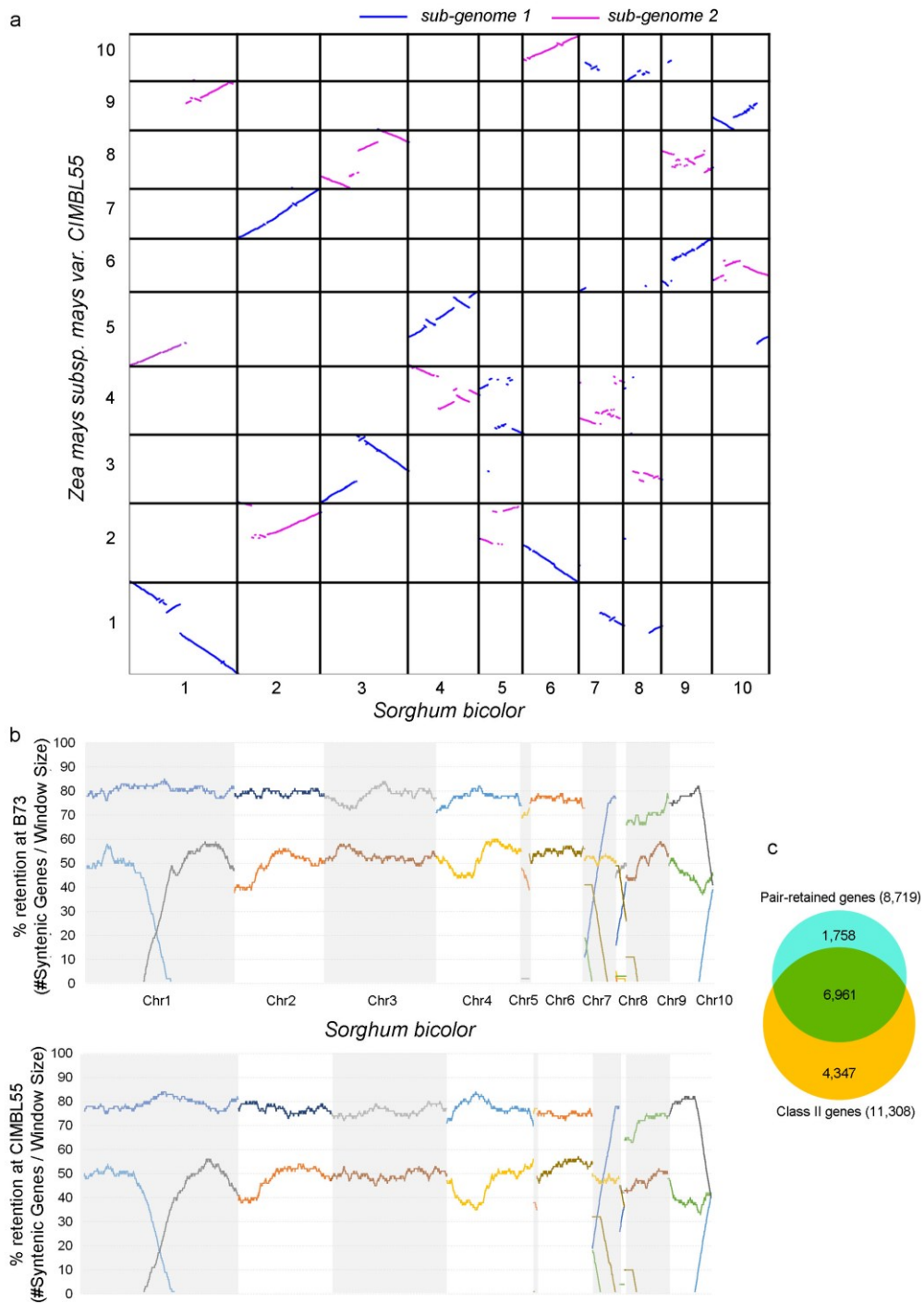
Supplementary Figure 1. Survival rate (%) and grain yield (g) of B73, CIMBL55 and Mo17 in a drought stress assay. Survival rate (%) for (a) B73 vs. CIMBL55, (b) Mo17 vs. CIMBL55, (c) B73 vs. Mo17. Eighteen plants of each genotype were used in each assay, and the assay was conducted three times. (d) Grain yield (g) per ear for CIMBL55, B73, and Mo17 under well-watered and water deficit conditions. Numbers in the parentheses denote the sample size used in the statistical analysis. Data represent the mean \pm SD. Statistical significance was determined by a two-sided *t*-test.



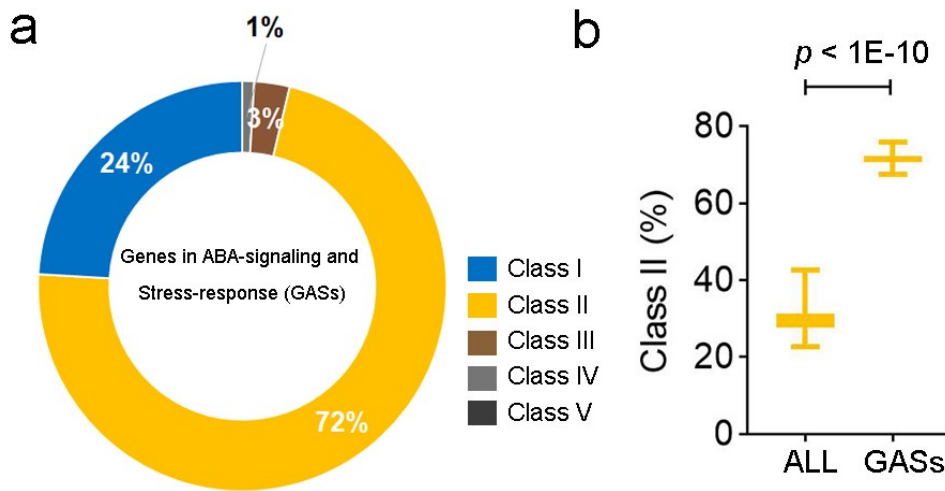
Supplementary Figure 2. Synteny analysis of the CIMBL55 and B73 genomes. Syntenic sequences longer than 10 Kb are indicated by grey lines. Translocations (purple), inversions (green), and duplications (orange) longer than 100 Kb are also indicated.



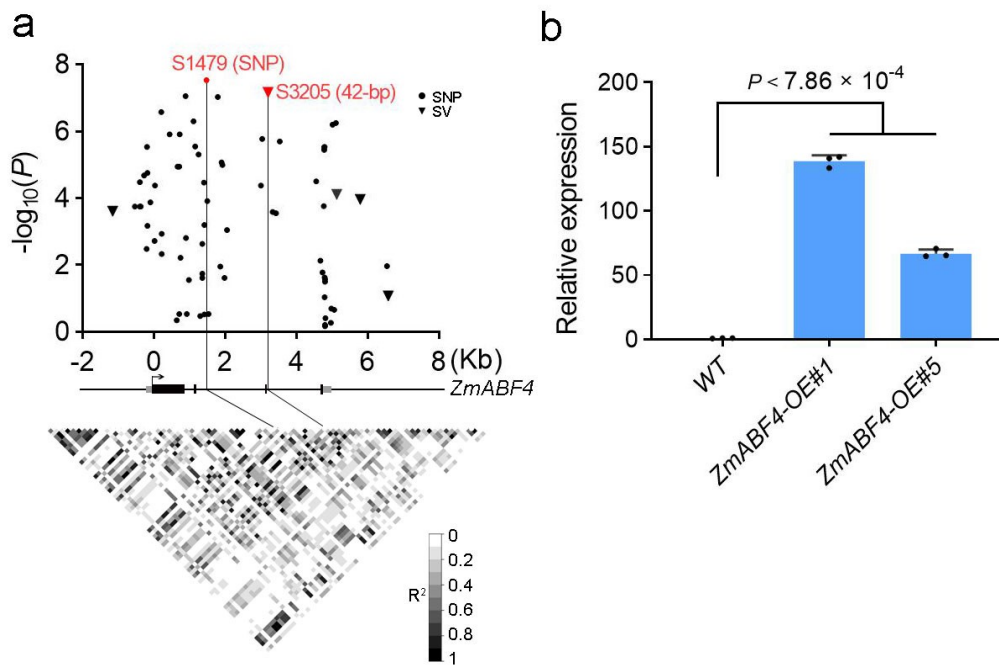
Supplementary Figure 3. Structural landscape of the CIMBL55 genome. (a) genes, (b) DNA-TEs, (c) RNA-TEs, (d-f) SNPs, insertions, and deletions, respectively, predicted using MUMMer software after bi-directional filtering, (g-i) mCG, mCHG, and mCHH density, respectively in a sliding window of 1Mb. The tracks are intensity-coded. The greater the color intensity, the higher the frequency of each element. (j) gene expression level in seedling leaves under well-watered (WW), in blue, and water stress (WS), in pink, conditions²⁷.



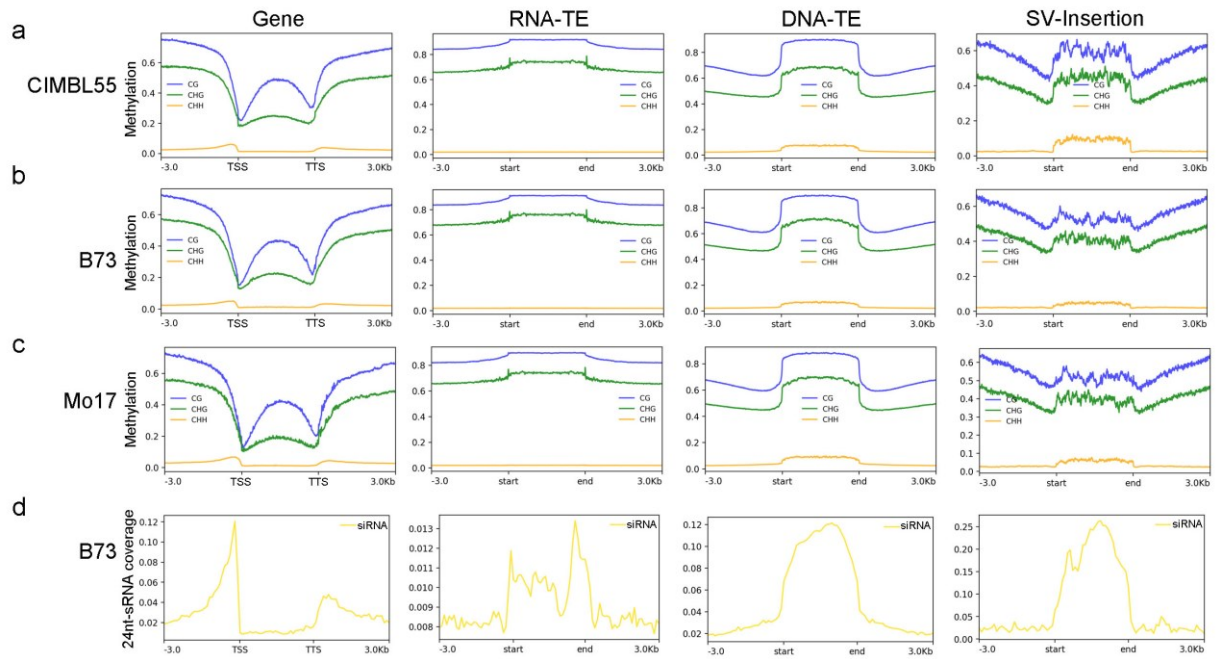
Supplementary Figure 4. Sub-genomic division and fractionation bias analysis of CIMBL55. (a) the two sub-genomes of CIMBL55. Blue for maize sub-genome 1 and pink for sub-genome2. (b) Fractionation bias analysis of CIMBL55 and B73 referring to the sorghum genome. Different colors are used to distinguish different sub-genomic fragments. (c) Overlap of pair-retained genes with Class II synteny genes in CIMBL55.



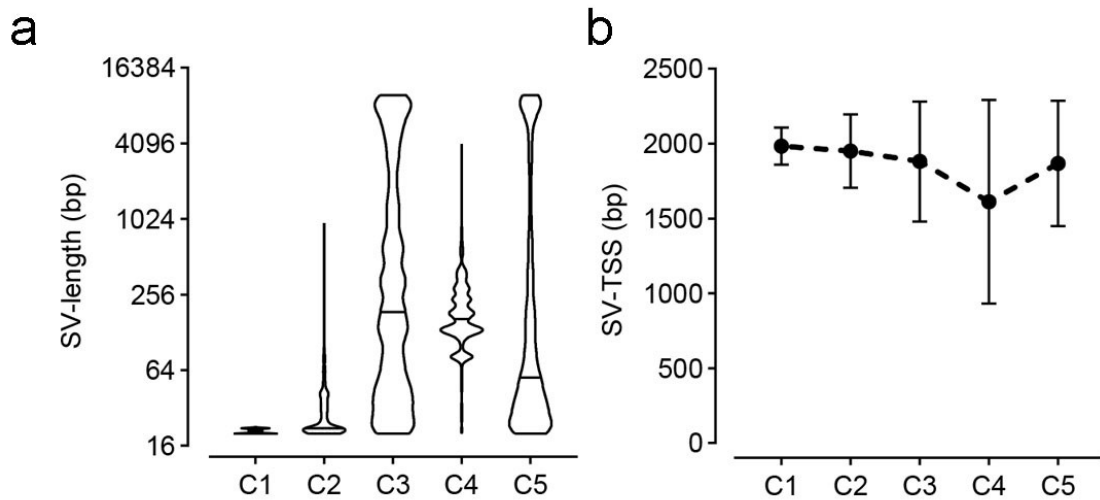
Supplementary Figure 5. Genes involved in ABA-signaling and stress-response (GASs) were enriched in Class II syntenic genes. (a) Distribution of GASs among Class I-V genes in CIMBL55. (b) GASs were significantly enriched in Class II genes. The significance was indicated by a two-sided *t*-test of difference between the percentages of Class II gene from gene set of the whole genome or GASs, based on 1000 permutations with random selection. Data represent the mean \pm SD.



Supplementary Figure 6. Analysis of the genetic variants of *ZmABF4* and their contribution to drought resistance. (a) *ZmABF4*-based association mapping for its expression level under well-watered (WW) condition. (b) Relative expression level of *ZmABF4* in WT and two *ZmABF4*-overexpressing lines, OE#1 and OE#5. Data represent the mean \pm SD, based on three biological replicates. Statistical significance was determined by a two-sided *t*-test.



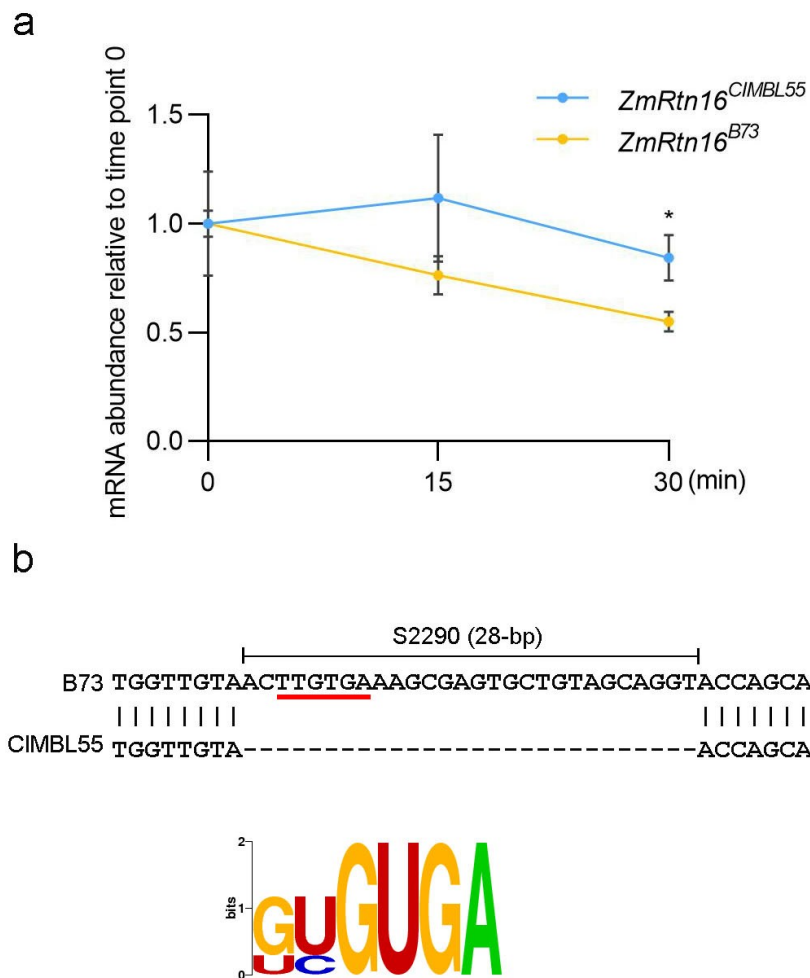
Supplementary Figure 7. Profile of CG, CHG, CHH methylation in the gene, RNA-TE, DNA-TE, and insertional regions in the CIMBL55(a), B73 (b), and Mo17 (c) genomes. (d) Profile of 24-nt sRNA in the B73 genome.



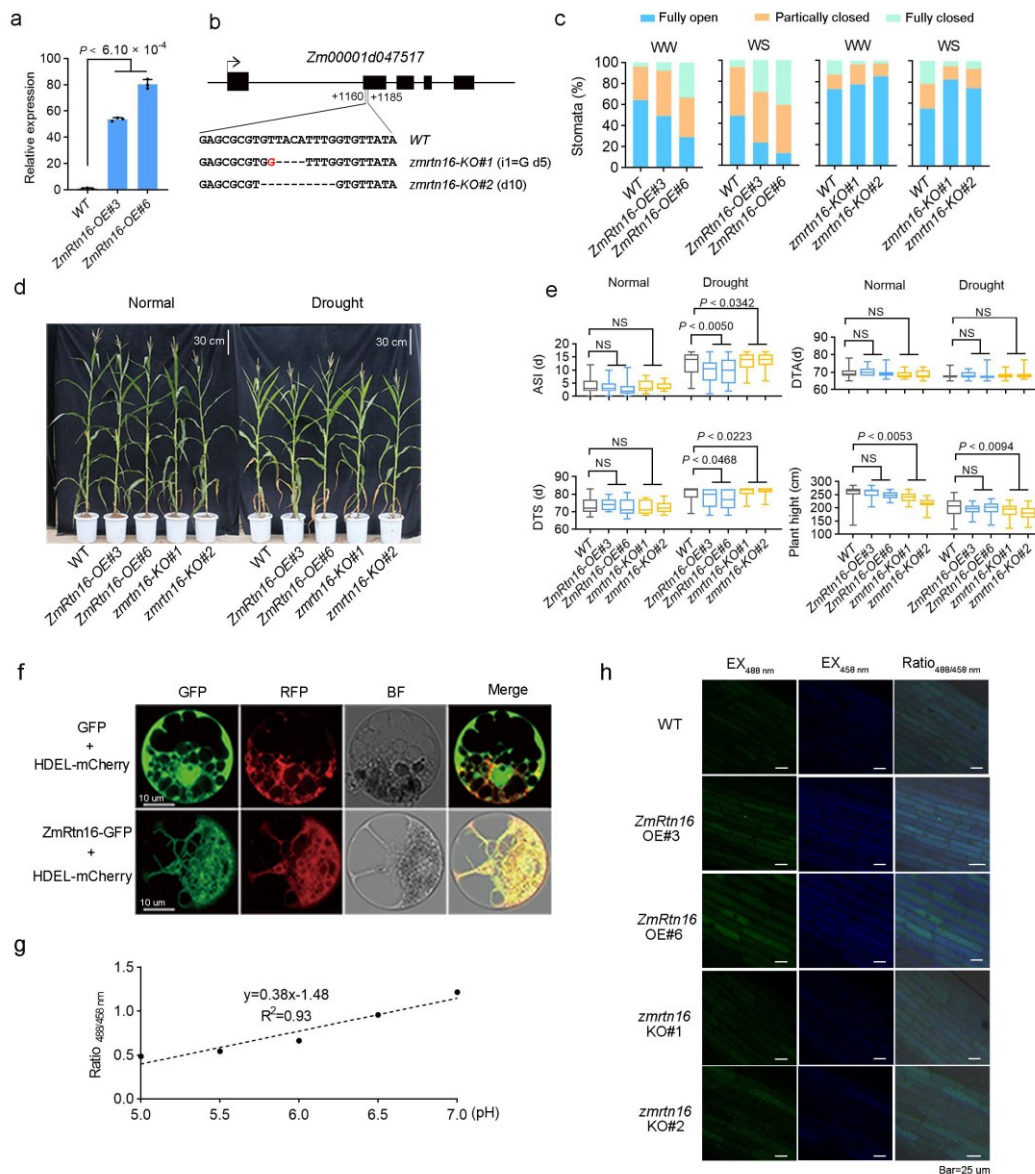
Supplementary Figure 8. Structural features of the five clusters (determined by hierarchical clustering analysis) of SV-related differential methylation regions (DMRs) identified in CIMBL55. (a) Violin plot illustrating the length of insertions (SV-length). (b) Mean value of the distance from an SV to a transcriptional start site of the closest gene (SV-TSS). Data represent the mean \pm SD.



Supplementary Figure 9. Schematic diagram of the CRISPR-targeted knockout (KO) genotype of *Zmdrd1*.

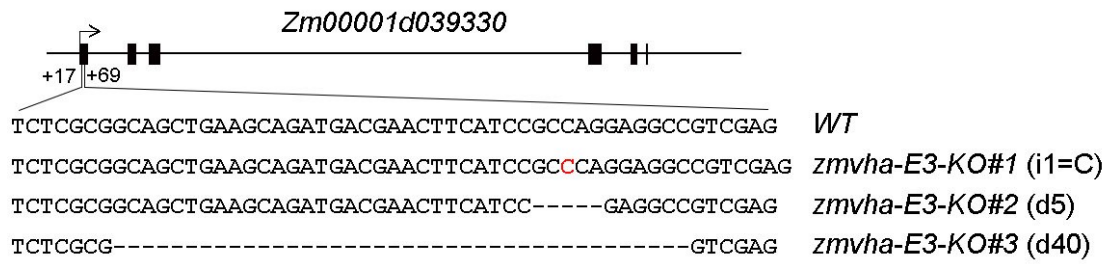


Supplementary Figure 10. The mRNA decay assay and putative motif analysis of RNA-binding proteins within the 28-bp insertion in the 3'-UTR of *ZmRtn16*^{B73}. (a) The mRNA abundance after the treatment of a transcription inhibitor (Triptolide), relative to the level of before the treatment. The experiments are performed independently twice with similar results. The data are from one representative results. Data represent the mean \pm SD from three biological replicates. Statistical significance was determined by a two-sided *t*-test. (b) A putative RNA motif recognized by RNA-binding proteins was identified in the sequence of the 28-bp insertional sequence.



Supplementary Figure 11. Functional analysis of *ZmRtn16*. (a) Relative expression of *ZmRtn16* in WT and two independent *ZmRtn16*-overexpressing (OE) lines under well-watered conditions. Data represent the mean \pm SD, based on three biological replicates. Statistical significance was determined by a two-sided *t*-test. (b) Schematic diagram of the *ZmRtn16* CRISPR-knockout (KO) genotype. (c) Percentage of fully open, partially closed, and fully closed stomatal apertures in *ZmRtn16* OE and KO plants under well-watered (WW) conditions and after a 5h dehydration (WS) treatment. (d) The morphology of *ZmRtn16* OE and KO plants grown under normal (well-watered) and drought conditions. The plants were photographed after anthesis and silking. Scale bar,

30 cm. (e) Histogram of the anthesis and silking interval (ASI), days to anthesis (DTA), days to silking (DTS), and plant height in WT, and two OE and two KO lines under normal (well-watered) and drought conditions in the field. Data represent the mean \pm SD of at least 15 plants (normal conditions) and 47 plants (drought conditions) for each genotype. Statistical significance was determined by a two-sided *t*-test. (f) Subcellular localization of ZmRtn16-GFP protein. HDEL-mCherry was the endoplasmic reticulum marker that was used. Representative photos were shown based on 12 observations. Scale bar, 10 μ m. (g) Calibration curve for the determination of vacuolar pH. Root samples soaked in a serial of standard equilibration buffers (pH value from 5.0 to 7.0) were analyzed to make a calibration curve. (h) Images show the emission intensities of root epidermal cells of WT, *ZmRtn16*-OE and -KO plants, stained with BCECF (2',7'-bis-(2-carboxyethyl)-5-(and-6)-carboxyfluorescein). The sample were excited with the lasers at 488 nm and 458 nm. Representative photos were shown based on at least 9 measurements from 6 seedlings for each plant type. Scale bar, 25 μ m.



Supplementary Figure 12. Schematic diagram of the CRISPR-targeted knockout (KO) genotype of *ZmVHA-E3*.